ADVANCES IN MATERIALS SCIENCE, Vol. 18, No. 2 (56), June 2018

DOI: 10.1515/adms-2017-0029

J. Łabanowski*, M. Jurkowski, M. Landowski

Gdansk University of Technology, Faculty of Mechanical Engineering, Department of Materials Science and Welding Engineering, 11/12 Narutowicza, 80-233 Gdańsk, Poland
*jlabanow@pg.edu.pl

THE EFFECT OF LONG TERM SERVICE AT ELEVATED TEMPERATURES ON MICROSTRUCTURE DEGRADATION OF AUSTENITIC REFORMER TUBES

ABSTRACT

The paper analyses the relationship between an increase of the inner diameter of tubes made of Manaurite XM cast steel and transformations occurring in their microstructure due to long-lasting operation in methane reformer. Examinations included metallographic analysis with light microscope (LM), scanning electron microscope (SEM) and microanalysis of the chemical composition of precipitates (EDX). It was indicated that there is a relationship between the microstructure degradation ratio, morphology of the precipitates and an increase of the inner diameter of the tubes.

Keywords: *Manaurite XM, reformer tubes, Fe-Ni-Cr alloy, carbides, degradation*

INTRODUCTION

Creep-resistant austenitic cast steel Manaurite XM is used in production of centrifugally cast tubes of catalytic methane reformers. A methane reformer usually contains 40 – 400 catalytic tubes whose length reaches 16 m at outer diameter ranging from 100 to 150 mm and tube wall thickness is 10 mm. Chemical conversion reaction between methane and water steam proceeds in the catalytic tubes producing a mixture of hydrogen, carbon oxide and carbon dioxide. Conversion reaction occurs in tubes filled with nickel catalyst on a porous ceramic carrier in temperatures ranging from 800°C to 950°C and pressure of 3÷4 MPa. Heat necessary to trigger the process is delivered from the outside by means of gas heaters which directly heat the tube surfaces.

Calculated durability of catalytic tubes operating in such conditions usually amounts to 100,000 hours. Even a slight exceeding of the design assumptions, especially the ones concerning the temperature, results in significant shortening of the lifetime period of the reformer tubes [1÷3].

Usefulness of a material intended for catalytic tubes is determined by its high resistance to creep and the appropriate plasticity limit in the operating temperatures, a large reserve of plasticity in temperatures below the operating temperatures ensuring high resistance to

thermal impacts, high resistance to oxidizing and carbonizing. Such properties can be found in high-alloy chromium - nickel cast steel with austenitic structure. Most commonly, the tubes made of these cast steels are produced by centrifugal casting which gives the tube a coarse-grained columnar structure that is advantageous due to creep resistance. Apart from the increase of the dimension of the austenite grain, the creep resistance is determined by strengthening of the solid solution and the mechanism of dispersion strengthening – mostly the type and morphology of the precipitates of primary and secondary carbides on the boundaries and in austenite grains. Iron alloys containing 23-28% Cr, 23-38% Ni, 0.30-0.60% C and additives of niobium, titanium and vanadium are a standard material used for the production of catalytic tubes for conversion of methane with water steam. [1,3,4]

The composition of creep-resistant 4th generation cast steel, such as Manaurite XM, was selected in such a way as to ensure the optimum mechanical properties and high creep resistance. High content of nickel, reaching 35%, stabilizes the austenitic structure and decreases the probability of the occurrence of brittle σ (FeCr) phase in the microstructure. Maintaining the content of silicone at 1.0% ensures the production of a layer of oxides on the surface of the tubes. The oxides layers prevent the penetration of the tube structure with oxygen and carbon and, also, decrease the alloy susceptibility to the development of σ phase. The presence of niobium in the composition of creep-resistant cast steel is intended and is connected with the phenomenon of the synergistic effect of at least two micro-additives. Similarly to niobium, titanium builds carbides, however it is used in lower amounts. Addition of titanium hinders the development of G phase whose presence in the microstructure is detrimental, as is the presence of σ phase [5]. Phase G ($Nb_6Ni_{16}Si_7$) develops in the course of diffusion of niobium carbide NbC in temperatures ranging from 700°C to 900°C [6÷8].

The σ phase should not develop during the utilization of Manaurite XM cast steel due to high content of nickel, however, it can occur in case of the transformation of secondary carbides $M_{23}C_6$. The phase develops when temperatures range from 600°C to 950°C and it has the form of blocks or needles located along the boundaries of austenite dendrites [4, 9÷11]. Between a brittle σ phase and austenitic matrix and also between coagulated $M_{23}C_6$ carbides and alloy matrix, micro-discontinuities and creep pores can develop due to differences in structures between the phases [1, 12].

The operational durability of catalytic tubes depends on the stability of the alloy microstructure and propagation of the creep processes. Creep processes initiate the formation of pores on the interface of carbides and austenitic matrix which then develop and combine with adjacent pores forming micro-cracks and, in the final stage – macro-cracks.

A wide array of diagnostic methods aimed at assessing the condition of the tube during operation has been developed. In industrial conditions, non-destructive testing methods indicating the progress of the tube microstructure degradation are the most desirable. Creep wear is measured with the increase of the tube dimensions, including the increase of the tube diameter and circumference or the axial elongation. Measurement of the inner diameter of a tube and its outer circumference are most commonly used. In advanced stages of tube wear, the assessment of degradation consists in measuring the depth of creep cracks of the tubes with methods taking the advantage of eddy currents or ultrasounds [6,7,8].

The most reliable results are provided by destructive tests of tube elements after the operation. Accelerated creep tests allow the determination of the residual durability of a construction element with high degree of probability. However, these tests are rarely used due to lengthy duration and high prices. Metallographic examinations characterize the condition of the microstructure of elements after operation and are useful in comparing them with previously defined microstructural standards for a given alloy [1]. The results of destructive tests can be used to assess the condition of the tested tube, while generalization of these

results to all the tubes working in a reformer is only possible when it is certain that all the operational conditions (local temperature, volume of gas flow in a tube) are the same.

Applying varied criteria of the assessment of tube durability often yields discrepant results. A method which unambiguously describes the condition of material after operation and the possibility of its further usage has not been developed so far. This paper presents the results of the examination of the degradation of the microstructure of catalytic tubes made of Manaurite XM alloy. The tubes were removed from a reformer due to excessive increase of the inner diameter. A relationship between the increase of the inner diameter of a tube and the transformations in microstructure has been analysed.

EXAMINATIONS METHODOLOGY

The examinations have been carried out on two centrifugally casted tubes, marked A and B, made of austenitic cast steel Manaurite XM (G-X45NiCrNbTi35-25) originating from a methane reformer. The tubes whose outer diameter was 146 mm and wall thickness was 10 mm were built of 3 girth welded sections of combined length of 15.8 m. The tubes had been operating at inner pressure of 3.0 MPa and maximum outer surface temperature of 937°C. The operational durability of tubes in these conditions is 100,000 hours.

The examined tubes were retired from service after 41,000 hours of operation. Sections intended for examination were taken from the areas where the increase of the inner diameter was the largest. The exact locations are specified in Table 1.

Table 1. *Sections of catalytic tubes taken for the examinations*

Tube section marking	Distance from the upper flange of the tube, mm	Inner diameter increase %
A-0	200	0.00
A-1	11000	5.55
B-1	11000	3.16

Section marked as A-0 was treated as a reference material – without microstructure changes – due to low operating temperature in this section of the tube (not exceeding 540°C).

Chemical composition of the examined sections of tubes was determined with the aid of optical spectrometer. The results of the analysis of chemical composition of the examined tubes can be seen in Table 2.

Table 2. *Chemical composition of the examined sections of Manaurite XM austenitic cast steel catalytic tubes*

Specimen	Chemical composition wt.%									
	C	Si	Mn	P	S	Cr	Mo	Ni	Nb	Ti
Manaurite XM	0.40 0.45	1.20 2.00	max 1.50	max 1.030	max 1.030	23.0 27.0	max 0.50	32.0 35.0	0.50 1.00	+
A-0	0.53	2.05	1.30	0.012	0.001	25.2	0.10	36.7	0.67	0.05
A-1	0.53	2.00	1.25	0.011	0.001	25.9	0.09	36.8	0.68	0.04
B-1	0.53	2.06	1.18	0.008	0.001	24.1	0.06	37.0	0.71	0.03

Data listed in Table 2 above indicate that each section of the tubes have a chemical composition characteristic for Manaurite XM (G-X45NiCrNbTi3525) cast steel and probably originate from the same heat.

Alloy microstructure was examined with Leica MEF4 light microscope. The specimens were mechanically polished and etched with Murakami reagent (30 g $K_3Fe(CN)_6$, 30 g KOH, 60 ml water).

The specimens for microscopic metallographic examinations were also examined with a Hitachi scanning electron microscope coupled with EDAX energy-dispersive X-ray spectroscope. The specimens were examined at x500 magnification. Chromium and niobium carbides were observed in BSE images. In order to define the distribution of elements in carbides and matrix of the cast steel within the selected area, elemental mapping of chromium, iron, silicone, molybdenum and nickel. The analysis of the chemical composition of micro-areas was conducted at accelerating voltage of 15 kV, registering the results of the X-ray spectra and chemical composition tables.

RESULTS

Figures 1-3 show the images of the microstructures of the examined tunes observed with a light microscope and scanning electron microscope.

Microstructure of A-0 section does not indicate any degradation traits. It is composed of austenitic matrix and carbide-austenitic eutectic system of characteristic, lamellar composition located on the boundaries of austenite grains. Apart from the eutectic system, there are also elongated primary carbides distributed along the austenite boundaries (Fig. 1a, b). There are no secondary precipitates in the austenite grains visible in the microstructure.

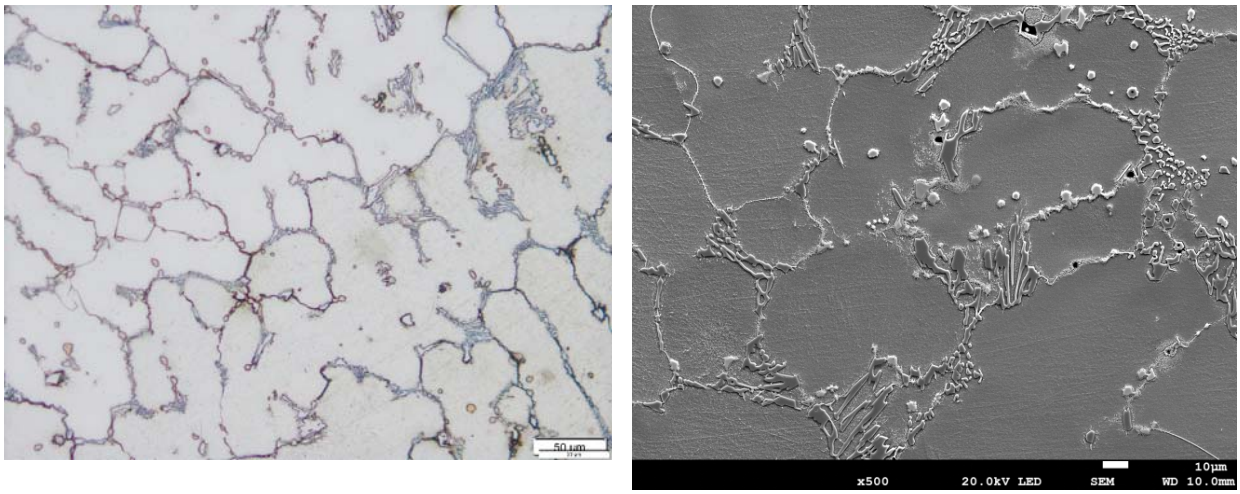

Fig. 1. Microstructure of Manaurite XM cast steel. Specimen A-0, non-degraded structure: a) LM, b) SEM

A-1 section microstructure exhibits advanced features of degradation. A complete disintegration of carbide eutectic system occurred. Large, coagulated primary carbides distributed along the austenite boundaries and creating locally continuous network can be seen. A limited number of quite large secondary carbides which have already been coagulated (Fig. 2) can be seen within austenite grains.

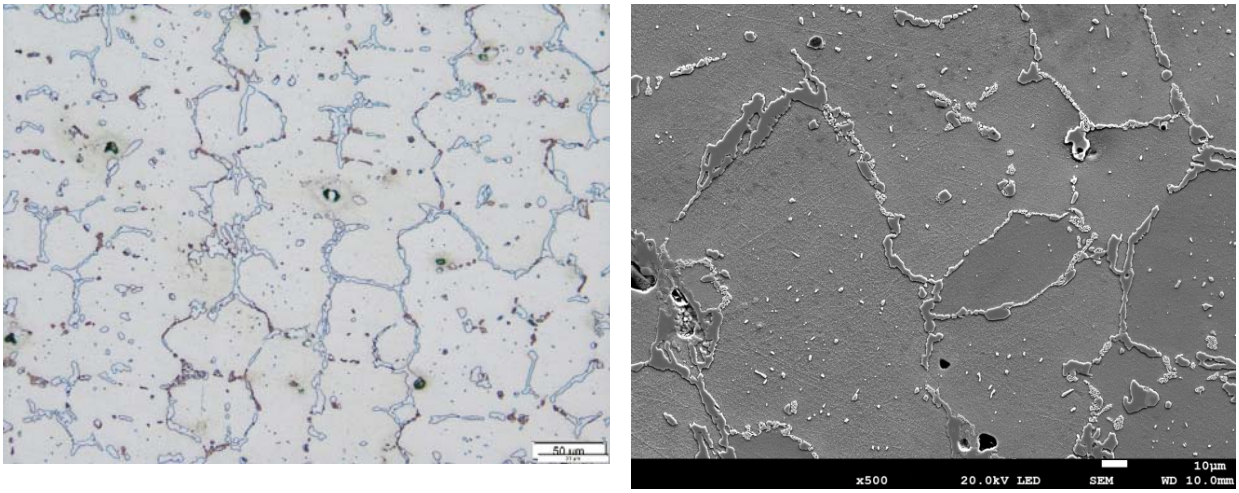

Fig. 2. Microstructure of Manaurite XM cast steel. Specimen A-1, degraded structure: a) LM, b) SEM

B-1 section microstructure also exhibits advanced features of degradation. A complete disintegration of carbide eutectic system occurred. Large aggregations of coagulated carbides with rounded edges are visible. Numerous precipitates of small secondary carbides distributed irregularly within austenite grains, Fig. 3, are also visible. The degree of the coagulation of secondary carbides is still low.

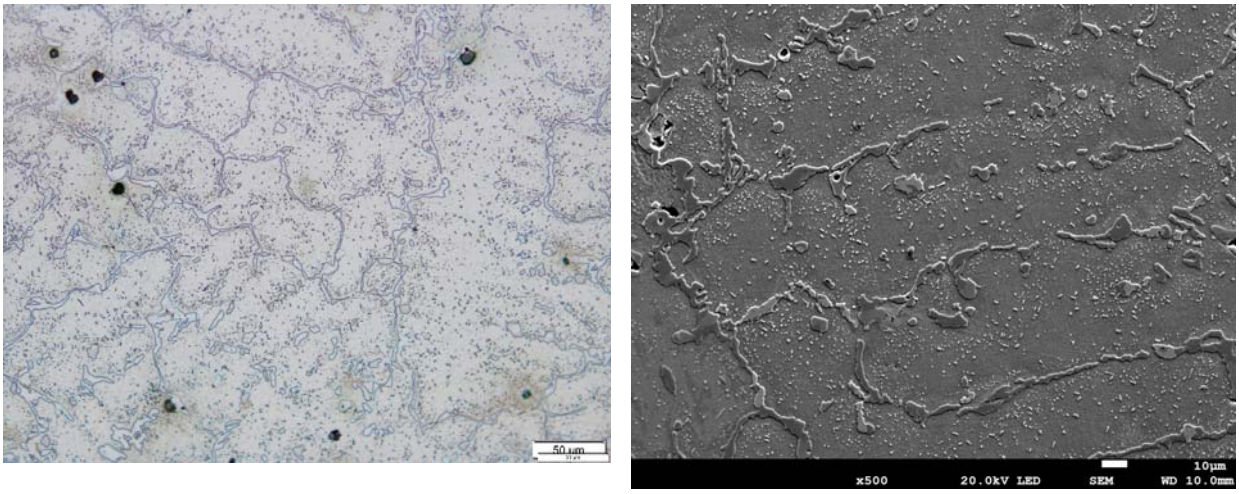

Fig. 3. Microstructure of Manaurite XM cast steel. Specimen B-1, degraded structure: a) LM, b) SEM

Metallographic examinations aiming at exposing the presence of discontinuities in the structure of the specimens in the form of micro-cracks or creep pores were conducted. Initial analysis was performed by observing etched specimens with a light microscope. However, analysis of etched specimens can be misleading due to carbide chipping which occurs during polishing and subsequent deep etching of these areas. More exact examinations were performed on non-etched specimens examined with a scanning electron microscope (SEM). The results of these examinations can be seen in Fig. 4. A-0 section microstructure does not exhibit creep pores nor micro-cracks, however, creep micro-pores were found in A-1 and B-1 tube section microstructures. The occurrence of micro-pores was more intense in A-1 section. The micro-pores were located in 1/3 of the tube thickness from its inner side. Areas where micro-pores are arranged in the form short strings directed perpendicularly to the tube axis were observed in A-1 section.

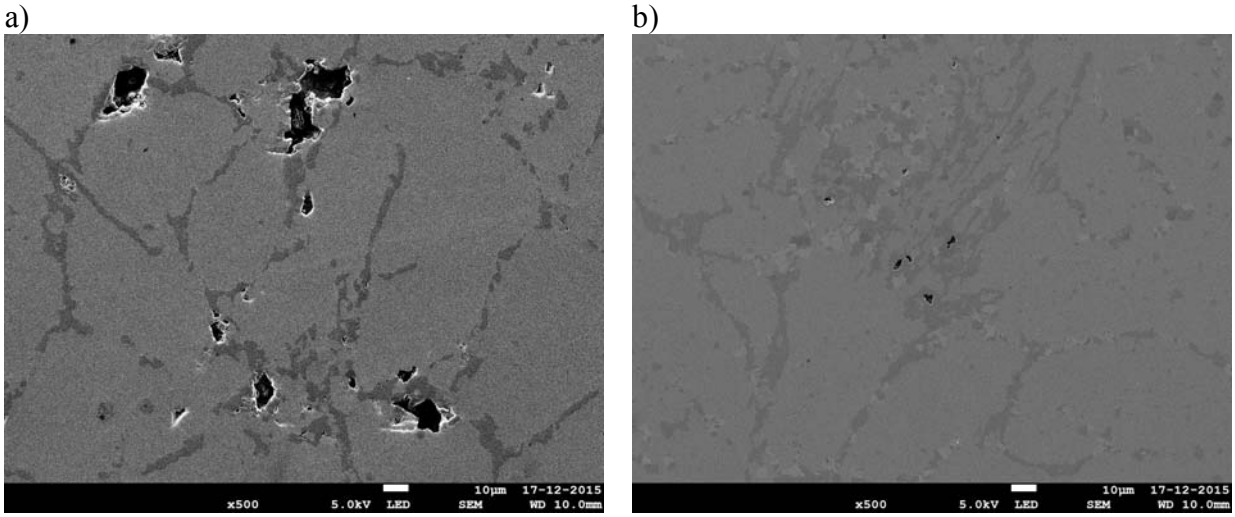

Fig. 4. Creep pores visible in the structure of Manaurite XM cast steel: a) specimen A-1. b) specimen B-1, SEM images, non-etched specimens.

Microanalysis of the chemical composition of precipitates

Figure 5 presents the superficial distribution of elements in A-0 specimen microstructure. The analysis of the eutectic system components indicates that lamellar precipitates of primary carbides contain chromium and lower amounts of niobium. The composition of chromium carbides includes also iron, nickel and silicone.

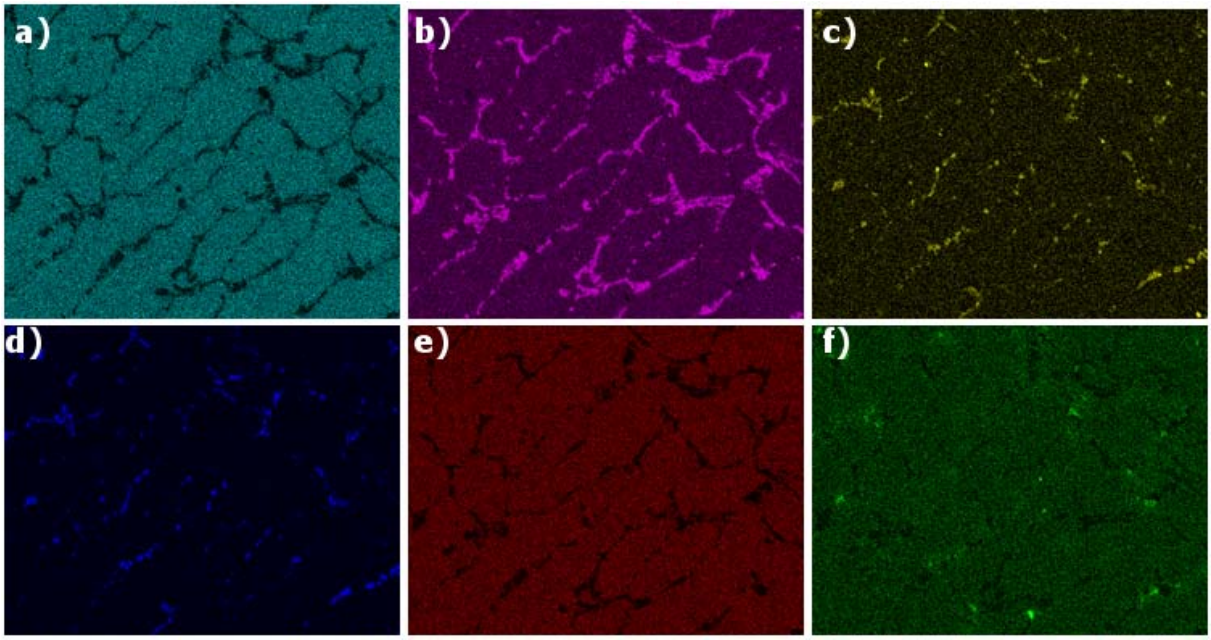

Fig. 5. Superficial distribution of elements in A-0 specimens: a) iron, b) chromium, c) molybdenum, d) niobium, e) nickel, f) silicone

Eutectic carbides (primary) are large and have clearly defined edges of shapes, figure 6a-c. Spot microanalysis of the chemical composition showed that – in majority – they are chromium carbides M_7C_3 (fig. 6a, b) and, also, rare, brighter, spherically shaped carbides rich in niobium, probably NbC (fig. 6c). A bright phase in the form of small, bright needles

appears in the vicinity of primary chromium carbides, fig. 6d. Field analysis of this area indicated an increased content of chromium. It is probably the area where first precipitates of secondary carbides similar to $M_{23}C_6$ are being formed.

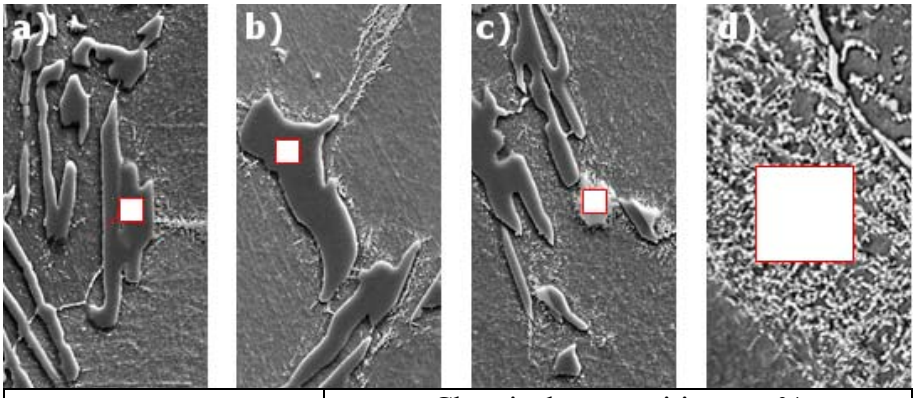

Area shown in figure	Chemical composition, wt.%						
	Fe	Cr	Nb	Ni	Si	Mn	Ti
6a	10.9	86.5	-	2.6	-	-	-
6b	11.2	85.9	-	2.9	-	-	-
6c	-	3.2	87.9	-	-	0.4	7.3
6d	30.6	26.7	-	37.9	4.8	-	-

Fig. 6. Microanalysis of the chemical compositions of the Manaurite XM cast steel components, wt.%. Specimen A-0

Figure 7 presents the back scattered electron (BSE) SEM image of the microstructure of degraded specimen A-1. Coagulated chromium carbides, type $M_{23}C_6$ can be seen on austenite grain boundaries as dark precipitates, while phases rich in niobium, probably type $Nb_6Ni_{16}Si_7$, are visible as bright precipitates. Precipitates shapes have slightly rounded edges which differentiates them from the ones present in A-0 specimen. The differences in the chemical composition of these precipitates can be seen in figure 8a, b. Spherical precipitates within the austenite grains, figure 8c, d are type $M_{23}C_6$ carbides which mostly contain chromium. Intermetallic phases type σ have not been found.

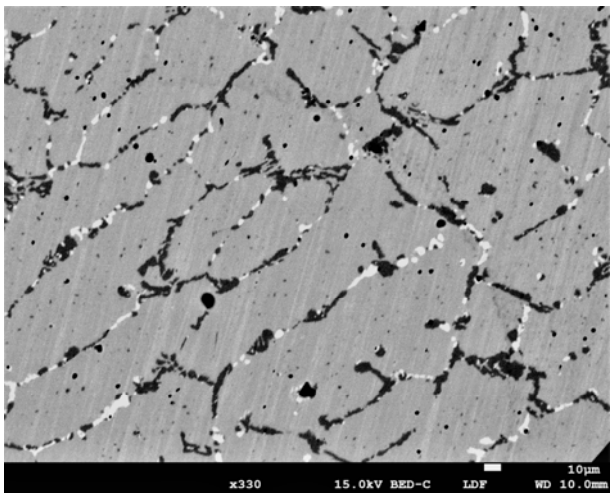

Fig. 7. Microstructure of A-1 specimen. SEM, back scattered electrons (BSE)

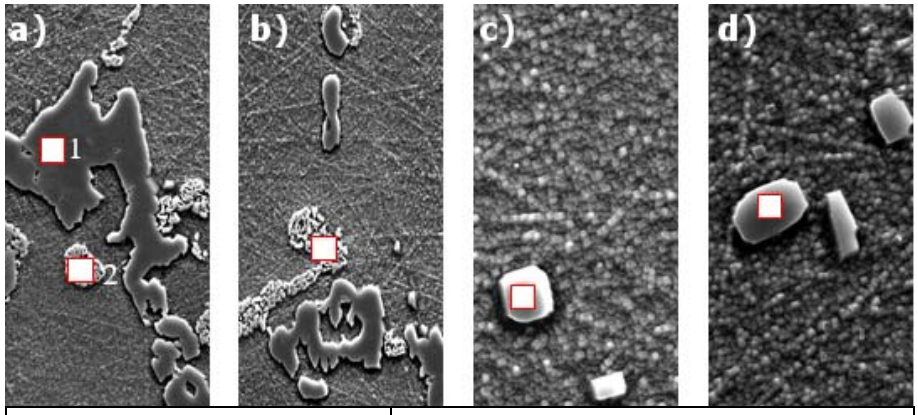

Area shown in figure	Chemical composition, wt.%				
	Fe	Cr	Nb	Ni	Si
8a-1	12.0	81.6	-	6.4	-
8a-2	21.8	15.4	32.8	24.6	2.0
8b	22.2	16.2	33.3	25.4	2.3
8c	14.7	76.0	-	8.8	0.6
8d	12.6	79.9	-	7.0	0.6

Fig. 8. Microanalysis of the chemical compositions of the Manaurite XM cast steel components, wt.%. Specimen A-1

Precipitates on the boundaries of the austenite grains in specimen B-1 are similar to the ones visible in A-1 specimen, fig. 9a, b. Figure 9d presents the images of secondary precipitated carbides in austenitic matrix. Their chemical composition corresponds the equilibrium composition of chromium carbide type $M_{23}C_6$ in Cr-Ni (76% Cr, 15% Fe, 4% Ni) cast steels. However, precipitates in the form of blocks with lower content of chromium and high content of iron (fig. 9c) have been found which indicates the proceeding process of the transformation of $M_{23}C_6$ carbides into intermetallic σ phase characterising with significant brittleness.

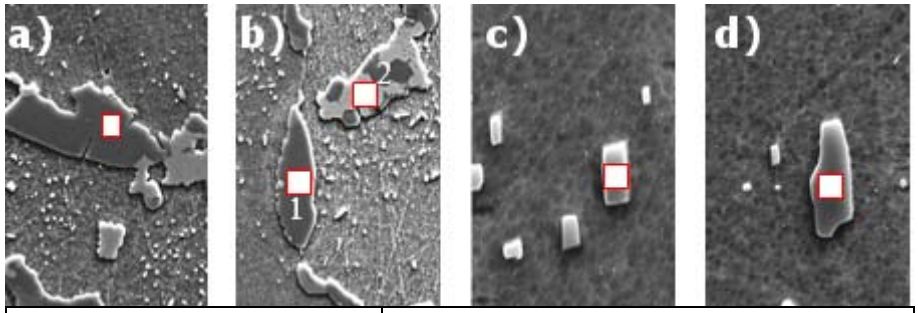

Area shown in figure	Chemical composition, wt.%				
	Fe	Cr	Nb	Ni	Si
8a	8.1	87.3	-	4.5	-
8b-1	8.0	87.3	-	4.6	-
8b-2	4.7	3.8	30.4	48.3	12.1
8c	22.4	59.5	-	17.0	1.0
8d	13.7	76.3	-	9.4	0.6

Fig. 9. Microanalysis of the chemical compositions of the Manaurite XM cast steel components, wt.%. Specimen B-1

SUMMARY

Conducted metallographic examinations of the sections of catalytic tubes made of Manaurite XM cast steel allow assessing the microstructure degradation ratio as advanced, corresponding the period of the secondary stage of steady-state creep. Considering the operational period amounting to 41% of the anticipated operational durability, it can be stated that the progress of degradation had an excessive character. This is also indicated by the ratios of the tube inner diameter increase which are 3.16% and 5.55%.

There were no features of degradation in reference material taken near the tube flange where the temperature had not exceeded 540°C. There was no inner diameter decrease in this section of the catalytic tube.

The areas where the microstructure degradation ratio was the highest were located in the medium sections of the tubes where, probably, an excessive increase of the temperature occurred. At the section below 1/3 of the length from the flange, catalytic tubes should operate at fixed thermal conditions, at the assumed operating temperature. Operational conditions, especially exceeding the maximum temperature of the tube wall, define the progress of the microstructure degradation. Exceeding the tube operational temperature might have been caused by improper adjustment of the heaters, poor condition of the catalyst or low mechanical resistance of the catalyst carrier.

There were no creep pores found in A-0 reference specimen, however, they were present in the microstructures of both A-1 and B-1 specimens. In A-1 specimen characterized by the highest increase of the inner diameter, there were areas where micro-pores start to form short strains directed perpendicularly to the tube axis. Isolated creep pores were found in B-1 specimen.

Secondary precipitates within the austenite grains occur in A-1 and B-1 specimens, however, they are not visible in A-0 reference specimen. Microstructure degradation ratio in specimens featuring an increase of the inner diameter is varied. A-1 specimen with the highest increase of the inner diameter has the most advance degradation degree. Degradation progress is accompanied by the changes of morphology, number and type of secondary precipitates in cast steel structure [13, 14]. In A-1 specimen the secondary precipitates within the grains of austenite are coagulated and their number is lower than in B-1 specimen. Apart from niobium and chromium carbides, A-1 and B-1 specimens featured phases rich in niobium, nickel and silicone, probably $Nb_6Ni_{16}Si_7$ type.

CONCLUSIONS

- Conducted metallographic examinations indicated a significant microstructure degradation ratio, excessive in relation to the service life of the tubes.
- There is a correlation between an increase of the diameter and microstructure degradation ratio. Microstructure degradation progresses with the increase of the inner diameter of the tubes.
- There were no microcracks whose presence would indicate the termination of the steady-state creep, the duration of which is considered to be the acceptable duration of the safe operation. The number of creep micro-pores increases and their arrangement changes with the degradation progress.

- A probable cause of the premature degradation of the microstructure of examined tube was an excessive increase of the temperature resulting from the poor condition of the catalyst.
- Long-lasting operation of the tubes in increased temperature causes the changes in precipitates morphology. Coagulation and a decrease of the number of secondary precipitates within austenite grains occur. There are also processes of transforming carbides into phases rich with niobium, nickel and silicone.

REFERENCES

1. Łabanowski J., Assessment of catalytic tubes degradation of reformer units in service. Gdansk University of Technology, Gdansk 2003 (in Polish).
2. Łabanowski J., Jurkowski M., Landowski M., Effect of Long Term Service at Elevated Temperatures on Mechanical Properties of Manaurite XM Reformer Tubes. Advances in Materials Science, 16(4) (2016) 38÷44.
3. Le May I., da Silveira T. L., Vianna C. H.: Criteria for the evaluation of damage and remaining life in reformer furnace tube. International Journal of Pressure Vessels and Piping 66 (1996) 233÷241.
4. Ray A. K., Sinha S. K., Tiwari Y. N., Swaminathan J., Das G., Chaudhuri S., Singh R.: Analysis of failed reformer tubes. Engineering Failure Analysis, 10 (2003) 351÷362.
5. Manoir Industries: http://www.manoir-industries. com/site/docs_wsw/fichiers_communs/docs/MI_Manaurite_XM.pdf
6. Wen S., Xuezhi Q., Jianting G., Langhong L., Lanzhang Z.: Microstructure stability and mechanical properties of a new low cost hot-corrosion resistant Ni-Fe-Cr based superalloy during long-term thermal exposure. Materials and Design, 69 (2015) 70÷80.
7. Wahab A. A., Hutchinson C. R., Kral M. V., Three-dimensional characterization of creep void formation in hydrogen reformer tubes. Scripta Materialia, 55 (2006) 69÷73.
8. Alvino An., Lega D., Giacobbe F., Mazzocchi V., Rinaldi A.: Damage characterization in two reformer heater tubes after nearly 10 years of service at different operative and maintenance conditions. Engineering Failure Analysis, 17 (2010) 1526÷1541.
9. Chen Q. Z., Thomas C. W., Knowles D. M., Characterisation of 20Cr32Ni1Nb alloys in as-cast and Ex-Service conditions by SEM, TEM and EDX. Materials Science and Engineering A, 374 (2004) 398÷408.
10. Sustaita-Torres I. A., Haro-Rodriguez S., Guerrero-Mata M. P., de la Garza M., Valdes E., Deschaux-Beaume F., Colas R.: Aging of a cast 35Cr-45Ni heat resistant alloy. Materials Chemistry and Physics, 133 (2012) 1018÷1023.
11. Łabanowski J.: Evaluation of reformer tubes degradation after long term operation. Journal of Achievements in Materials and Manufacturing Engineering, 43 (1) (2010) 244÷251.
12. Lee J. H., Yang W. J., Yoo W. D., Cho K. S., Microstructural and mechanical property changes in HK40 reformer tubes after long term use. Engineering Failure Analysis, 16 (2009) 1883÷1888.
13. Kondrat'ev S.Y., Kraposhin V.S., Anastasiadi G.P., Talis A.L., Experimental observation and crystallographic description of M7C3 carbide transformation in Fe-Cr-Ni-C HP type alloy. Acta Materialia, 100 (2015) 275÷281.
14. Laigo J., Christien F., Le Gall R., Tancret F., Furtado J., SE, EDS, EPMA-WDA and EBSD characterization of carbides in HP type heat resistant alloys. Materials Characterization, 59 (2008) 1580÷1586.